JOURNAL OF ENGINEERING SCIENCES

Volume 11, Issue 1 (2024)

Ivanchuk Y. V., Belzetskyi R. S., Ozeranskyi V. S., Khomenko V. M., Dobrovolska K. V. (2024). Modeling of wave processes in hydraulic drive systems of technological equipment. Journal of Engineering Sciences (Ukraine), Vol. 11(1), pp. D19–D26. https://doi.org/10.21272/jes.2024.11(1).d3

Modeling of Wave Processes in Hydraulic Drive Systems of Technological Equipment

Ivanchuk1 Y. V.[1*][0000-0002-4775-6505], Belzetskyi R. S.[1][0000-0003-1574-8831], Ozeranskyi V. S.[1][0009-0007-1694-2317], Khomenko V. M.[1][0009-0007-7943-4299], Dobrovolska K. V.[2][0000-0001-9517-1723]

[1] Vinnytsia National Technical University, 95, Khmelnytske Hwy., 21021, Vinnytsia, Ukraine;
[2] National Pirogov Memorial Medical University, 56, Pyrohova St., 21018 Vinnytsia, Ukraine

Article info:

Submitted:	October 3, 2023
Received in revised form:	December 11, 2023
Accepted for publication:	December 19, 2023
Available online:	January 10, 2024

***Corresponding email:**
ivanchuck@vntu.edu.ua

Abstract. The article, based on the performed theoretical research, solves the essential scientific and technical problem of increasing the accuracy of identification of wave processes in a hydrodynamic system (pipeline) by developing a generalized method of mathematical designing of the dynamics of a continuous viscous and weakly compressed fluid in the hydrodynamic system pipeline based on the Navier-Stokes equation. Amplitude-frequency characteristics represent parameters of wave processes in the hydraulic drive system. A partial solution of Navier–Stokes equations, under zero initial conditions, is proposed in the form of four-pole equations, the components of which are represented in the form of the Laplace image of the corresponding relative pressure and flow coordinates and the the hydraulic line parameters determine the four-pole elements themselves It is also proposed to determine the values of the four-pole elements based on time constants and relative damping coefficients on the frequency characteristics of hydraulic lines with distribution parameters based on the condition of equality of the first resonant frequencies and amplitudes (at these frequencies). With the help of the developed methods, the primary dynamic parameters of the amplitude-frequency characteristics of continuous viscous and weakly compressed liquid in the pipeline of hydraulic systems for different flow ranges. This made it possible to achieve the following practical results: the high degree of adequacy of the developed mathematical model indicates an increase in the reliability of determining the operating characteristics when designing a hydraulic drive. The high accuracy of determining the first resonant frequencies and amplitudes allows for creating a hydraulic pump with improved operational characteristics.

Keywords: vibration, operating fluid, Navier–Stokes equations, amplitude-frequency response, resonance mode.

1 Introduction

The hydraulic drive was widely used in technological equipment due to its simplicity, reliability in operation, low metal consumption, and optimal load parameters on the operating body [1]. The structural characteristics of the hydraulic drive and its components are mainly determined based on the implementation of the kinematic and power parameters of the executive body in the mode of its operating and free movements. The experience of operating machine-building technological equipment [2] shows that using static and kinematic requirements during design is insufficient. It was determined that vibrations occur in the hydraulic system of metal-operating technological equipment under external influence, which causes unstable speed of movement of operating units and, as a result, additional oscillations occur on the executive body [3]. All this causes a general decrease in the reliability of technological equipment and a deterioration in the quality of the work performed. A sharp change in power and a high frequency of operation of a hydraulic drive with multiple operating parameters complicates the design and research of technological equipment. Analyzing the ambiguity of the dynamic properties of hydraulic drive elements shows the fundamental complexity of the mathematical description of hydrodynamic processes. Thus, the modern hydraulic drive of technological equipment is classified as a complex dynamic object, for the effective study of which, it is advisable to use mathematical and computer modeling [4].

The parameters of hydraulic lines significantly impact the dynamic characteristics of hydraulic equipment. Frequently, there are vibrations in hydraulic equipment, which is a consequence of the coincidence of resonance frequencies of oscillations of hydraulic lines with hydraulic devices connected to the hydraulic system and with frequencies of external periodic influences. Therefore, considering the frequency characteristics of hydraulic lines when designing hydraulic systems of technological equipment is a necessary condition for developing hydraulic systems with a reduced vibration level [5].

Mathematical modeling of work processes in various technological devices is widely used. It allows for investigating the impact of design and mode factors on the main characteristics of the device to outline specific ways to improve them while significantly reducing the volume of experimental research. Despite the complexity of the calculations and assumptions in the mathematical description of the work process, which can be defined as experimental data accumulation, the perspective and relevance of using mathematical modeling to study hydrodynamic processes in the hydraulic system are apparent [6].

2 Literature Review

The physical parameters of the energy carrier (operating fluid) and its nodes' structural parameters significantly influence the hydraulic drive's speed, energy saturation, and compactness [7]. This leads to the development of mathematical models in the form of systems of differential equations of motion of structural elements of the hydraulic drive based on an artificial dynamic model with reduced coefficients for the oscillating system. The given coefficients describe the elastic-viscous characteristics of the hydraulic link based on the mathematical model of Kelvin–Focht [8] with further linearization of the dynamic properties, namely the assumption of constancy of the combined modulus of elasticity, density, and dynamic viscosity of the operating fluid, and this leads directly to disregarding wave processes [9] in the hydraulic drive itself. In turn, the existing differential equations with distributed coefficients are supplemented by differential equations of flow rates [10] in partial integral solutions of non-discontinuity and Navier–Stokes differential equations for an ideal operating fluid [11].

The practical implementation of such an approach is possible only for mathematical models of mostly low dimensionality. It describes the properties of objects in a narrow range of changes in such operating parameters as the amplitude and frequency of oscillation of hydraulic drive elements. Moreover, this leads to the limitation of the area of use of the results of mathematical modeling, which do not take into account the influence of all transient processes in the hydraulic circuit [12], which leads to the accumulation of excess, not implemented by the systems of technological movements [2–4].

In [13], an original method of "particles in cells" was proposed, which combines the advantages of the Lagrangian and Euler approaches [14]. The solution area in this method is divided by a fixed (Eulerian) grid. However, the continuous medium is interpreted by a discrete model – a set of "particles" of fixed mass (Lagrangian grid of particles) that move through the Eulerian grid of cells is considered. Particles determine the parameters of the fluid itself (mass, energy, velocity), while the Euler grid determines the parameters of the field (pressure, density, temperature). This method makes it possible to study complex phenomena in the dynamics of multicomponent environments; particles follow free surfaces and boundaries of environments. However, this method's main drawback is the solid medium's discrete representation, which results in numerical instability (fluctuations). It is also difficult to obtain information for regions of significant rarefaction, where virtually all particles leave.

In works [15, 16], a numerical method was developed concerning (ψ, ω) – the system of equations for the current function ψ and the vortex ω. A general drawback of these methods is the use of a boundary condition for a vortex on a solid surface in one form or another, which is absent in the physical formulation of the problem.

An additional iterative process associated with this boundary condition limits the speed of convergence of numerical algorithms. In addition, the apparent limitation of the solution methods for the (ψ, ω) system is associated with the impossibility of their development in the case of spatial flows of a viscous liquid and compressed gas flows.

One of the current scientific problems in hydromechanics is the description of the motion of a viscous, weakly compressed fluid, which is described by the continuity and Navier-Stokes equations [4, 10, 11]. These include fluid movement problems during laminar and turbulent flow around bodies of finite dimensions, currents in the wake zone and areas of flow disruption, and mixing and boundary layers at the body surface [17].

The nonlinearity of the Navier-Stokes equations and the presence of small parameters in their higher derivatives create difficulties, both in analytical research and in the numerical integration of these equations using computer systems. Thus, the problem of developing methods for solving the system of continuity and Navier-Stokes equations with high accuracy (especially in the multidimensional case), which will allow studying wave processes [18] in hydraulic systems of technological systems, remains an urgent task.

The presented research aims to improve the accuracy of identification of wave processes in hydraulic systems of technological machines by developing and implementing new, more efficient mathematical modeling. This will help achieve several qualitative practical results: increasing the reliability of determining performance characteristics when designing a hydraulic drive, the possibility of developing systems with improved performance characteristics, and reducing the time required to develop specific technologies.

To achieve the aim, the following tasks were solved:

– to develop a mathematical model of the dynamics of continuous viscous and weakly compressed fluid in the pipeline of hydraulic systems;

– to develop methods for solving the mathematical model of the dynamics of a continuous viscous and weakly compressed fluid in hydraulic lines, which will allow determining the parameters of wave processes in hydraulic systems;

– to determine the main dynamic parameters of continuous viscous and weakly compressed fluid in the pipeline of hydraulic systems for different flow ranges.

3 Research Methodology

A system with distributed parameters can represent a hydraulic line when modeling wave processes. The basic equations of unsteady fluid motion are the Navier-Stokes differential equations [10–12]. The following assumptions can be used when using the Navier-Stokes equations: for subsonic velocities, convective terms of nonlinear transport acceleration can be neglected [19].

Since the fluid velocity in the longitudinal direction is much greater than in the radial direction, the pressure across the cross-section can be taken constant; the fluid density ρ is taken constant and is determined depending on the average value of the set pressure.

Then, when studying the dynamic processes in the hydraulic line (Figure 1), Navier–Stokes equations can be written for small increments in the following form:

$$\begin{cases} -\frac{\partial(\Delta p)}{\partial x} = \frac{\rho}{S_T}\frac{\partial(\Delta q)}{\partial t} + r\Delta q; \\ \frac{\partial(\Delta p)}{\partial x} = -\frac{S_T}{E}\frac{\partial(\Delta q)}{\partial t}, \end{cases} \quad (1)$$

where $\Delta p = p_2 - p_1$ – pressure difference imposed on the set pressure p_0, Pa; $\Delta q = q_2 — q_1$ – flow difference imposed on the set flow rate q_0, m^3/s; x – linear coordinate of the hydraulic line, m; S_T – constant cross-section area, m^2; d_T – diameter, m.

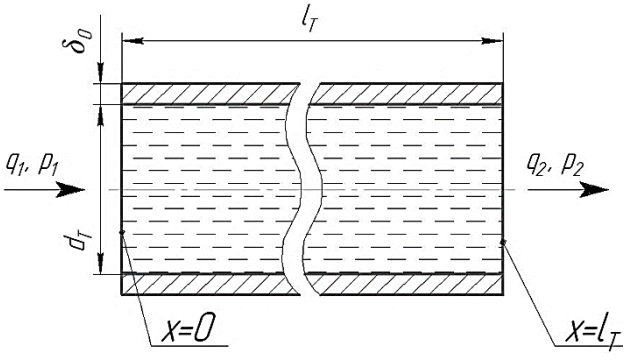

Figure 1 – The design scheme of dynamic processes in a hydraulic line

Equation (1) contains the cost coefficient [20]:

$$r = \frac{\Delta p}{l_T q_0} = \frac{\lambda q_0 \rho}{2 d_T F_T^2},$$

where λ – coefficient of resistance to the movement of the operating fluid from the action of internal friction forces [21].

The coefficient r characterizes the viscous friction loss per unit length of the nozzle attributed to the fluid flow rate.

Equation (1) also contains the modulus of elasticity:

$$E = E_0 / \left(1 + \frac{d_T E_0}{\delta_0 E_m}\right),$$

where E_0, E_m – the modulus of elasticity of the fluid and the material of the pipe walls, respectively, N/m^2; δ_0 – thickness, m.

The component $r\Delta q$ is responsible for the fluid viscosity caused by the velocity gradient in the flow direction, while the velocity gradient across the cross-section is neglected.

The system of partial differential equations (1) determines the dynamic characteristics of the hydraulic line depending on the parameters $\frac{\rho}{S_T} r$ and $\frac{S_T}{E}$, distributed along its length.

For the entire length l_T of the hydraulic line, the following parameters express the fluid inertia, resistance, and capacitance of the hydraulic line, respectively:

$$L_T = \frac{\rho l_T}{S_T};\ R = r l_T;\ C_l = \frac{S_T l_T}{E}.$$

The solution of the system of equations (1) at zero initial conditions can be represented in the form of four-pole equations [22]:

$$\begin{cases} P_1 = A_T(s) P_2 + B_T Q_2; \\ P_1 = C_T(s) P_2 + D_T Q_2, \end{cases} \quad (2)$$

where $A_T(s)$, $B_T(s)$, $C_T(s)$, and $D_T(s)$ – the elements of the four-pole, determined by the parameters of the hydraulic line; P_1, P_2, Q_1, and Q_2 – Laplace images of the corresponding relative coordinates of pressure and flow at the beginning ($x = 0$) and at the end ($x = l_T$) of the hydraulic line (Figure 1):

$$P_1 = L\left[\frac{\Delta p_1(t)}{p_{10}}\right];\ P_2 = L\left[\frac{\Delta p_2(t)}{p_{20}}\right];$$

$$Q_1 = L\left[\frac{\Delta q_1(t)}{q_{10}}\right];\ Q_2 = L\left[\frac{\Delta q_2(t)}{q_{20}}\right].$$

The system of equations (2) can be rewritten in the following matrix form:

$$\begin{bmatrix} P_1 \\ Q_1 \end{bmatrix} = G(s) \begin{bmatrix} P_2 \\ Q_2 \end{bmatrix}, \quad (3)$$

with the condition $A_T(s) D_T(s) - B_T(s) C_T(s) = 1$ and the following matrix:

$$G(s) = \begin{bmatrix} A_T(s) & B_T(s) \\ C_T(s) & D_T(s) \end{bmatrix}.$$

The structural diagram of the hydraulic line according to the system of equations (2) is presented in Figure 2.

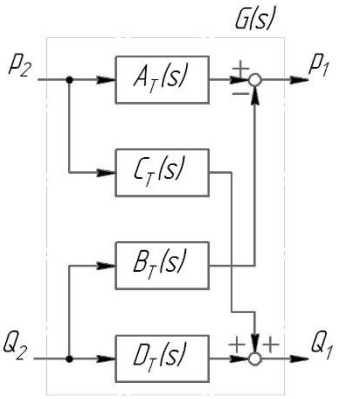

Figure 2 – The structural diagram of the hydraulic line in the form of four-pole equations

For the system of equations with distributional parameters (1) with the assumptions made, the elements of the system of equations (2) are as follows:

$$\begin{cases} A_T(s) = \frac{p_{20}}{p_{10}} l_T ch(\Gamma(s)); \\ B_T(s) = \frac{q_{20}}{q_{10}} l_T Z_C(s) sh(\Gamma(s)); \\ C_T(s) = \frac{p_{20}}{q_{10}} \frac{1}{Z_C(s)} l_T sh(\Gamma(s)); \\ D_T(s) = l_T ch(\Gamma(s)), \end{cases}$$

where $\Gamma(s) = \frac{1}{a}\sqrt{\left(\frac{F_T r}{\rho} + s\right)s}$ – the propagation constant of the wave process; $a = \sqrt{\frac{E}{\rho}}$ – the speed of sound in the operating fluid medium, m/s; $Z_c(s) = \sqrt{r + \frac{\rho}{F_T}s}$ – the characteristic resistance of the hydraulic line.

The frequency response of the hydraulic line is constructed by replacing the parameter s with $j\omega$, where j – imaginary unit ($j^2 = -1$).

In this case, the propagation constant of the wave process can be represented as $\Gamma(j\omega) = \gamma_1 + j\vartheta_1$, where the following conditions are met:

$$\frac{rS_T}{\omega\rho} \ll 1;\ \vartheta_1 = \frac{\omega}{a};\ \gamma_1 = \frac{1}{2}\frac{rS_T}{\sqrt{\rho E}}.$$

A study of the amplitude characteristics of the transfer matrix $G(s)$ elements shows that the resonant peaks' amplitudes do not change at successive frequencies. This result contradicts the experimental data [23] for the laminar flow of the operating fluid.

A significant discrepancy between theoretical and experimental results obtained from the system of equations (1) based on the assumptions made is explained by the fact that with an increase in the excitation frequencies, the effective resistance of a small-diameter hydraulic line, in laminar fluid flow, increases significantly, since the velocity profiles along the cross-section also change. This factor was not considered in the original system of differential equations (1), where losses during the oscillatory process in hydraulic lines were considered only through the coefficient r, determined from the steady-state flow characteristics.

Values of the components of the transfer matrix $G(s)$ provided that the hydraulic lines have a small diameter and taking into account the velocity gradient across the cross-section under the laminar steady-state regime [24]:

$$\begin{cases} A_T(s) = \frac{p_{20}}{p_{10}} l_T \cos\left(\frac{s\eta l_T}{a}\right); \\ B_T(s) = -\frac{q_{20}\rho_a \eta}{q_{10} S_T} \sin\left(\frac{s\eta l_T}{a}\right); \\ C_T(s) = \frac{p_{20} S_T}{q_{10}\rho a \eta} \sin\left(\frac{s\eta l_T}{a}\right); \\ D_T(s) = l \cos\left(\frac{s\eta l_T}{a}\right), \end{cases} \quad (4)$$

where $\eta = \gamma_2 + j\vartheta_2$ – a complex frequency function determined by a complex expression of Thomson functions depending on the parameter $\aleph = \frac{d_T}{2}\sqrt{\frac{\omega}{\nu}}$; ν – the kinematic viscosity, m^2/s.

If we separate the real part γ_2 and the imaginary part ϑ_2 of the function, it can be got:

$$\gamma_2 = \frac{\sin\left(\frac{1}{2}arctg\frac{n}{m}\right)}{(m^2+n^2)^{\frac{1}{4}}};\ \vartheta_2 = -\frac{\cos\left(\frac{1}{2}arctg\frac{n}{m}\right)}{(m^2+n^2)^{\frac{1}{4}}}, \quad (5)$$

where with an error that does not exceed 1 %, and for $\aleph \geq 4.0$, the value of $n = \frac{\sqrt{2}}{\aleph}\left(\frac{8\aleph - 3\sqrt{2}}{8\aleph + \sqrt{2}}\right)$, and $m = \frac{\sqrt{2}}{\aleph} - 1$.

The frequency responses of the elements $A_T(j\omega)$ and $D_T(j\omega)$ from the system of equations (4) show that at frequencies $\omega_i = \frac{i\pi a}{2l_T|\vartheta_2|_{\omega=\omega_i}}$ (i = 1, 3, 5, …), the amplitude responses have resonant peaks defined by the expressions:

$$\begin{cases} |A_T|_{\omega=\omega_i} = \frac{p_{20}}{p_{10}} sh\left(i\frac{\pi}{2}\left|\frac{\gamma_2}{\vartheta_2}\right|_{\omega=\omega_i}\right); \\ |D_T|_{\omega=\omega_i} = sh\left(i\frac{\pi}{2}\left|\frac{\gamma_2}{\vartheta_2}\right|_{\omega=\omega_i}\right), \end{cases}$$

where $\left|\frac{\gamma_2}{\vartheta_2}\right|_{\omega=\omega_i}$ – the ratio of the absolute values of γ_2 and ϑ_2 at the corresponding resonant frequencies.

Since the hydraulic lines of metal operating technological equipment are $i\frac{\pi}{2}\left|\frac{\gamma_2}{\vartheta_2}\right|_{\omega=\omega_i} \ll 1$ [25], these expressions can be written in the following form:

$$\begin{cases} |A_T|_{\omega=\omega_i} = \frac{p_{20}}{p_{10}} i\frac{\pi}{2}\left|\frac{\gamma_2}{\vartheta_2}\right|_{\omega=\omega_i}; \\ |D_T|_{\omega=\omega_i} = i\frac{\pi}{2}\left|\frac{\gamma_2}{\vartheta_2}\right|_{\omega=\omega_i}. \end{cases} \quad (6)$$

Similarly, the amplitude-frequency characteristics of the elements $B_T(j\omega)$ and $C_T(j\omega)$ have resonant peaks at frequencies $\omega_k = k\frac{\pi a}{l_T|\vartheta_2|_{\omega=\omega_k}}$ (k = 1, 2, 3, …):

$$\begin{cases} |B_T|_{\omega=\omega_k} = \frac{q_{20}}{p_{10}} \frac{\rho a|\eta|_{\omega=\omega_k}}{S_T} k\pi \left|\frac{\gamma_2}{\vartheta_2}\right|_{\omega=\omega_k}; \\ |C_T|_{\omega=\omega_k} = \frac{p_{20}}{q_{10}} \frac{S_T}{\rho a|\eta|_{\omega=\omega_k}} k\pi \left|\frac{\gamma_2}{\vartheta_2}\right|_{\omega=\omega_k}, \end{cases} \quad (7)$$

where $|\eta|_{\omega=\omega_k}$ – the modulus of the complex function $\eta = \gamma_2 + j\vartheta_2$ at $\omega = \omega_k$.

From expressions (6) and (7), it follows that the amplitudes of the resonant peaks of the frequency characteristics of the elements of the transfer matrix *G(s)* decrease at successive resonant frequencies with a slope of the derivative of 10,0 dB/dec, which is consistent with experimental data [23, 26].

A sufficiently accurate approximation of the frequency characteristics of the characteristics can be obtained using the transfer matrix *G(s)* with the following matrix elements [27]:

$$\begin{cases} A_T(s) = k_{T1}(T_{T1}^2 s^2 + 2\xi_{T1}T_{T1}s + 1); \\ B_T(s) = k_{T2}(T_{T3}s + 1)(T_{T2}^2 s^2 + 2\xi_{T2}T_{T2}s + 1); \\ C_T(s) = T_{T4}s(T_{T2}^2 s^2 + 2\xi_{T2}T_{T2}s + 1); \\ D_T(s) = T_{T1}^2 s^2 + 2\xi_{T1}T_{T1}s + 1. \end{cases} \quad (8)$$

The time constants T_{T1} and T_{T2} and the relative damping coefficients ξ_{T1} and ξ_{T2} are determined from the frequency characteristics of the hydraulic lines with the distribution parameters described by equations (4), based on the condition of equality of the first resonant frequencies and amplitudes (at these frequencies) of the characteristics of the corresponding elements $A_T(j\omega)$, $B_T(j\omega)$, $C_T(j\omega)$, and $D_T(j\omega)$ based on equations (4) and (8). Under these conditions, the following relations will be obtained [4, 8]:

$$\begin{cases} T_{T1} = \frac{2l_T}{\pi a}; \quad T_{T2} = \frac{l_T}{\pi a}; \\ \zeta_{T1} = \frac{\pi}{8} arctg \frac{2\sqrt{2T_{T1}\nu}}{d_T}; \quad \zeta_{T2} = \frac{1}{4} arctg \frac{2\sqrt{2T_{T2}\nu}}{d_T}; \\ T_{T3} = \frac{\rho}{S_T r}; \quad T_{T4} = \frac{p_{20}S_T l_T}{q_{10}E}; \\ k_{T1} = \frac{p_{20}}{p_{10}}; \quad k_{T2} = \frac{q_{20}}{p_{10}}R. \end{cases} \quad (9)$$

In the case when the range of significant frequencies of the processes studied in the hydraulic system is limited to $\omega \ll \frac{\pi a}{2l_T}$, the second-order differentiating links in the transfer matrix (8) can be neglected. Therefore, the following simplified transfer matrix can describe the dynamic characteristics of the hydraulic lines:

$$T_1 + T_4 = \frac{l_1 p_{10}}{E_0 v_0}\left(1 + \frac{E_{T1}l_{T1}}{S_1 l_1}\right). \quad (10)$$

Depending on the tasks under study, transfer functions of hydraulic lines of various types are used. The calculation and study of the dynamic characteristics of hydraulic systems can be carried out taking into account two types of influence: external forces on the operating body of mechanical engineering equipment and periodic changes in flow rates caused by the pulsation of the hydraulic pump supply to the hydraulic system.

In the case when the study is carried out under the influence of an external load, the transfer functions of the pressure and drain hydraulic lines are required [28, 29].

For a pressure hydraulic line, the input is the change in flow rate at its outlet Q_2, and the output is the change in pressure P_2. Accordingly, the transfer function of the pressure hydraulic line – $W_{T1}(s) = \frac{P_2}{Q_2}$. Therefore, from the system of equations (2) it can be obtained:

$$W_{T1} = \frac{B_T - \frac{P_1}{Q_1}D_T(s)}{-A_T + \frac{P_1}{Q_1}C_T(s)}, \quad (11)$$

where P_1/Q_1 is the transfer function of the element located at the inlet to the hydraulic line.

In order to take into account the dynamic characteristics of the drain hydraulic line in the calculation of the hydraulic system, a transfer function is required, the input of which is the change in flow at the beginning of the drain hydraulic line and the output coordinate is the change in pressure at this point. Accordingly, the transfer function of the drain hydraulic line can be represented as – $W_{T2}(s) = \frac{P_1}{Q_1}$.

From the system of equations (2) it can be obtained:

$$W_{T2} = \frac{A_T(s)\frac{P_2}{Q_2} + B_T(s)}{C_T(s)\frac{P_2}{Q_2} + D_T(s)}, \quad (12)$$

where P_2/Q_2 – the transfer function of the element located at the outlet of the drain hydraulic line.

When studying the response of hydraulic systems to the pulsating supply of a hydraulic pump, it is advisable to use a transfer function that determines the ratio of the change in pressure at the outlet of the hydraulic line to the change in pressure at its inlet:

$$\frac{P_2}{P_1} = \frac{1}{A_T(s) + B_T(s)\frac{Q_2}{P_2}}, \quad (13)$$

where Q_2/P_2 is the inverse transfer function of the element or apparatus at the outlet of the hydraulic line.

4 Results

Figure 3 shows the theoretical and experimental frequency characteristics [25, 30] of a hydraulic line made of copper pipes with an internal diameter of 15.0 mm, a wall thickness of 1.5 mm, and a length of 4.65 m at an installed pressure of p_{10} = 1.47 MPa.

The experimental and theoretical frequency characteristics $\frac{P_1(j\omega)}{Q_1(j\omega)}$ (Figure 4) were constructed based on equations (4) and (8) for the case of a throttle washer at the hydraulic line outlet using equation (12). The studies were carried out on a hydraulic line made of copper pipes with an internal diameter of 14.0 mm, a wall thickness of 2.0 mm, and a length of 3.2 m [22].

The frequency characteristics of hydraulic lines $P_2(j\omega)/P_1(j\omega)$, which correspond to equation (13) for similar conditions (Figure 4), are shown in Figure 5.

The presented results of the theoretical (equations (4) and (8)) and experimental studies (Figure 5) are also in good agreement with each other. In particular, the results measured up to natural frequencies of 180 Hz at a phase shift of –240° and up to natural frequencies of 100 Hz for the amplitude of natural oscillations within 7 dB are in good agreement. The accuracy of the corresponding mathematical model does not exceed 9 %.

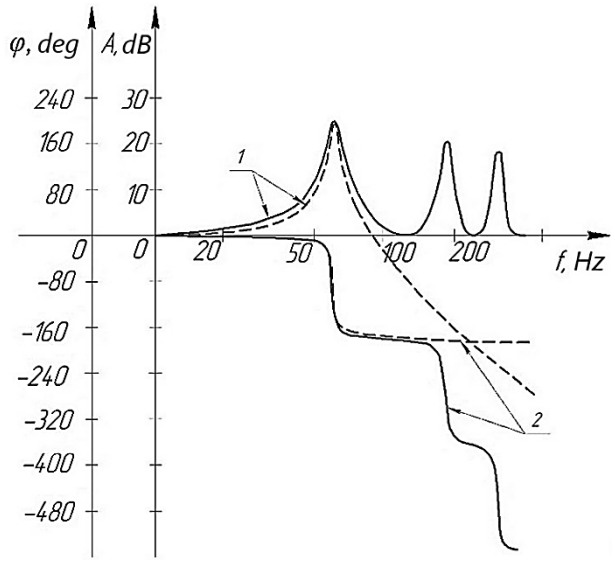

Figure 3 – Diagrams of hydraulic line frequency characteristics: 1 – change in the amplitude of oscillations of the operating fluid depending on its natural frequency; 2 – change in the phase of oscillations of the operating fluid depending on the natural frequency (solid line – experimental dependence; dashed line – theoretical dependence)

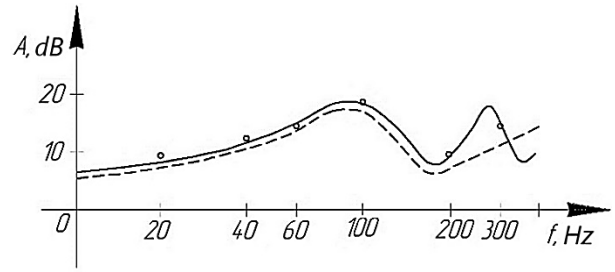

a

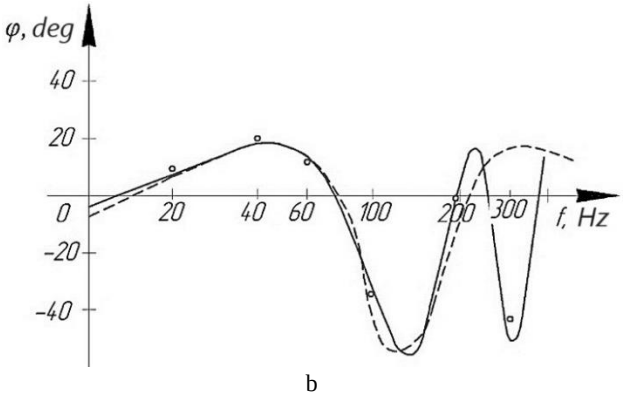

b

Figure 4 – Diagrams of hydraulic line frequency characteristics: a – change in the amplitude of oscillations of the operating fluid depending on its natural frequency; b – change in the phase of oscillations of the operating fluid depending on the natural frequency (solid line – theoretical dependence based on (4); dashed line – theoretical dependence based on (8); dot line – experimental dependence)

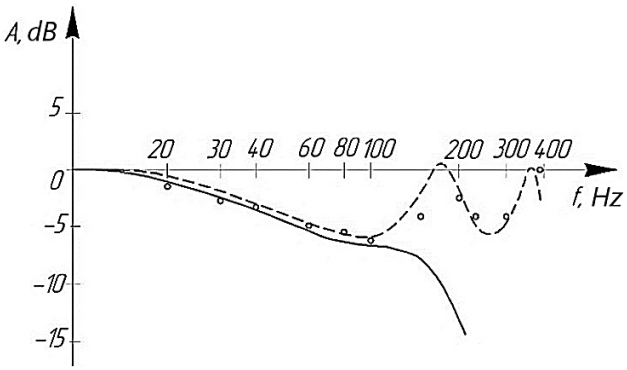

a

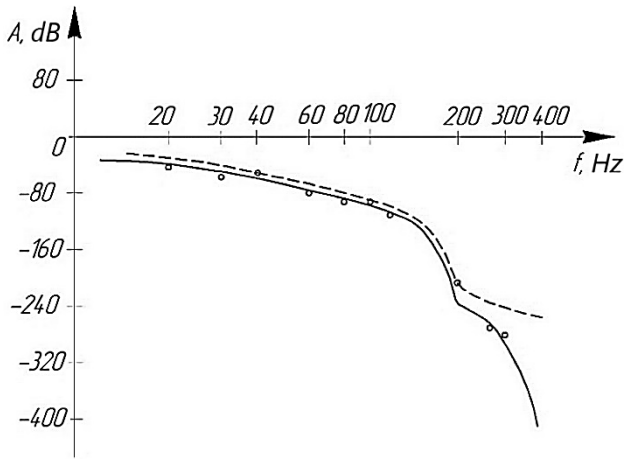

b

Figure 5 – Diagrams of hydraulic line frequency characteristics: a – change in the amplitude of oscillations of the operating fluid depending on its natural frequency; b – change in the phase of oscillations of the operating fluid depending on the natural frequency (solid line – theoretical dependence based on (4); dashed line – theoretical dependence based on (8); dot line – experimental dependence)

5 Discussion

The matching of the characteristics constructed (Figure 3) at the concentrated parameters with the experimental ones is satisfactory up to a frequency of 70 Hz, which covers the first resonant peak of 28 dB amplitude at a phase shift of 160°. The average accuracy of the developed mathematical model is 9 %.

Since the hydraulic lines of hydraulic drives of machine-building equipment are characterized by a small length at limited impact frequencies, in most cases, the dynamic characteristics can be considered only up to the first resonant frequency. In these cases, approximating these characteristics using the transfer matrix (8) gives accurate results for engineering calculations [8, 12].

The experimental study (Figure 4) of the frequency characteristics [3, 20] was carried out by imposing a sinusoidal effect on the curve of the set flow rate q_{10} = 32 l/min. The set pressure value at the beginning of the hydraulic line was p_{10} = 1.47 MPa, Reynolds number Re = 2100, the sound velocity in the operating fluid c_p = 1200 m/s, and kinematic viscosity $v = 2.5 \cdot 10^{-5}$ m^2/s.

Based on equations (4), the theoretical characteristics in Figure 4 were constructed. They are in good agreement with the experimental results. The approximated characteristics based on equations (8) also agree with the frequency covering the first resonant peak at 40 Hz with a phase shift of 20° and 90 Hz for a natural oscillation amplitude of 19 dB. The accuracy of the corresponding mathematical model is 9 %.

The discrepancy between the theoretical results (Figures 3–5) obtained from the mathematical model (1) under the assumptions made and the experimental data is explained by the fact that with an increase in the excitation frequencies, the effective resistance of a small-diameter hydraulic line under the laminar flow regime increases significantly since the velocity profiles along the cross-section of the pipes change.

The losses during the oscillatory process in a hydraulic line in laminar flow, considering the velocity gradient across the cross-section, increase since the profile of the velocity vectors ceases to have a parabolic shape. The velocity profiles also change under turbulent flow conditions (Re > 2300). Accordingly, matrix elements (4) must be adjusted for turbulent flow.

However, in most metal operating equipment, hydraulic lines with a turbulent flow regime are used only at very short lengths since losses in long lines increase intensively in turbulent flow [2, 8].

6 Conclusions

Based on theoretical studies, a significant scientific and technical problem of improving the accuracy of identifying wave processes in hydraulic system pipelines has been solved by developing a generalized method for mathematical modeling of the dynamics of a continuous viscous and slightly compressed fluid in a hydraulic system pipeline based on the Navier-Stokes equation.

A solution to the Navier–Stokes equation, at zero initial conditions, was proposed in the form of four-pole equations, the components of which are represented in the form of a Laplace image of the corresponding relative coordinates of pressure and flow, and the four-pole elements themselves were determined by the parameters of the hydraulic line.

The values of the four-pole elements were determined based on time constants and relative damping coefficients from the frequency characteristics of hydraulic lines with distribution parameters based on the condition of equality of the first resonant frequencies and amplitudes.

The developed methods allowed for evaluating the main dynamic parameters of the frequency characteristics for a continuous viscous and slightly compressed fluid in hydraulic systems (pipelines) for different flow ranges.

The accuracy of the developed mathematical model does not exceed 9 %.

References

1. Yakoubi, D. (2023). Enhancing the viscosity-splitting method to solve the time-dependent Navier–Stokes equations. *Communications in Nonlinear Science and Numerical Simulation*, Vol. 123, 107264. https://doi.org/10.1016/j.cnsns.2023.107264
2. Koval'chuk, R., Molkov, Y., Lenkovskiy, T., Grytsenko, O., Krasinskyi, V., Garbacz, T. (2018). Drive system parameters influence on run-up process of the drilling rig pumping unit. *Advances in Science and Technology Research Journal*, Vol. 12, pp. 199–206. https://doi.org/10.12913/22998624/100442
3. Manzhilevskyy, O.D. (2019). Analysis of hydraulic vibration drive machine for vibration abrasive processing. *Przeglad Elektrotechniczny*, Vol. 1(4), pp. 95–99. https://doi.org/10.15199/48.2019.04.16
4. Ivanchuk, Y., Manzhilevskyy, O., Belzetskyi, R., Zamkovyi, O., Pavlovych, R. (2022). Modelling of piling technology by vibroimpact device with hydropulse drive. *Scientific Horizons*, Vol. 25(1), pp. 9–20. https://doi.org/10.48077/scihor.25(1).2022.9-20
5. Jinjian, Z., Zhenyue, M., Xueni, W., Qianqian, W., Leike Z. (2023). Transient vibration of shafting in coupled hydraulic-mechanical-electrical- structural system for hydropower station during start-up process. *Applied Mathematical Modelling*, Vol. 124, pp. 860–880. https://doi.org/10.1016/j.apm.2023.08.041
6. Rukavishnikov, V.A., Rukavishnikov, A.V. (2023). Theoretical analysis and construction of numerical method for solving the Navier–Stokes equations in rotation form with corner singularity. *Journal of Computational and Applied Mathematics*, Vol. 429, 115218. https://doi.org/10.1016/j.cam.2023.115218
7. Parchei-Esfahani, M., Gee, B., Gracie, R. (2020). Dynamic hydraulic stimulation and fracturing from a wellbore using pressure pulsing. *Engineering Fracture Mechanics*, Vol. 235, pp. 107–152. https://doi.org/10.1016/j.engfracmech.2020.107152
8. Shatokhin, V.M., Sobol, V.N., Wyjcik, W., Mussabekova, A., Baitussupov, D. (2019). Dynamical processes simulation of vibrational mounting devices and synthesis of their parameters. *Przeglad Elektrotechniczny*, Vol. 4(19), pp. 86–92. https://doi.org/10.15199/48.2019.04.15
9. Kant, S., Munjal, M.L., Rao, D.L.P. (1974). Waves in branched hydraulic pipes. *Journal of Sound and Vibration*. Vol. 37(4), pp. 507–519. https://doi.org/10.1016/S0022-460X(74)80030-1
10. Iskovych-Lototsky, R.D., Ivanchuk, Y.V., Veselovska, N.R., Surtel, W., Sundetov, S. (2018). Automatic system for modeling vibro-impact unloading bulk cargo on vehicles. In: *Proc. SPIE 10808, Photonics Applications in Astronomy, Communications, Industry, and High-Energy Physics Experiments*, 1080860. https://doi.org/10.1117/12.2501526

11. Iskovych-Lototsky, R.D., Ivanchuk, Y.V., Veselovsky, Y.P., Gromaszek, K., Oralbekova, A. (2018). Automatic system for modeling of working processes in pressure generators of hydraulic vibrating and vibro-impact machines. In: *Proc. SPIE 10808, Photonics Applications in Astronomy, Communications, Industry, and High-Energy Physics Experiments*, 1080850. https://doi.org/10.1117/12.2501532
12. Zhang, Z. (2019). Wave tracking method of hydraulic transients in pipe systems with pump shut-off under simultaneous closing of spherical valves. *Renewable Energy*, Vol. 132, pp. 157–166. https://doi.org/10.1016/j.renene.2018.07.119
13. Harlow, F.H., Welch, J.E. (1965). Numerical calculation of time-dependent viscous incompressible flow of fluid with free surface. *Phys. Fluids*, Vol. 8(12), pp. 2182–2189.
14. Iskovych-Lototsky, R., Kots, I., Ivanchuk, Y., Ivashko, Y., Gromaszek, K., Mussabekova, A., Kalimoldayev, M. (2019). Terms of the stability for the control valve of the hydraulic impulse drive of vibrating and vibro-impact machines. *Przeglad Elektrotechniczny*, Vol. 4(19), pp. 19–23. https://doi.org/10.15199/48.2019.04.04
15. Amsden, A.A., Harlow, F.H. (1970). *The SMAC Method*. Los Alamos Scientific Lab., Rept. NLA-4370. Los Alamos, USA.
16. Easton, C.R. (1972). Homogeneous boundary conditions for pressure in MAC method. *J.Comput. Phys*., Vol. 9(2), pp. 375–379.
17. Ferras, D., Manso, P.A., Schleiss, A.J., Covas, D.I.C. (2017). Fluid-structure interaction in straight pipelines with different anchoring conditions. *Journal of Sound and Vibration*, Vol. 394, pp. 348–365. https://doi.org/10.1016/j.jsv.2017.01.047
18. Abramian, A.K. (2010). Wave propagation in a two-dimensional plane straight duct with panels embedded in its sidewalls. *Journal of Sound and Vibration*, Vol. 329(8), pp. 994–1006. https://doi.org/10.1016/j.jsv.2009.10.034
19. Hirmand, M.R., Vahab, M., Papoulia, K.D., Khalili, N. (2019). Robust simulation of dynamic fluid-driven fracture in naturally fractured impermeable media. *Computer Methods in Applied Mechanics and Engineering*, Vol. 357, pp. 112–574. https://doi.org/10.1016/j.cma.2019.112574
20. Zhiwei, Q., Xianghua, Y., Daozhi, W., Siwen, F., Qiuping, W. (2023). Physical model driven fault diagnosis method for shield Machine hydraulic system. *Measurement*, Vol. 220, 113436. https://doi.org/10.1016/j.measurement.2023.113436
21. Wilcox, D.C. (1988). Reassessment of the scale-determining equation for advanced turbulence models. *AIAA Journal*, Vol. 26(11), pp. 1299–1310. https://doi.org/10.2514/3.10041
22. Yan, R., Jian, R. (2016). Theoretical and experimental investigations of vibration waveforms excited by an electro-hydraulic type exciter for fatigue with a two-dimensional rotary valve. *Mechatronics*, Vol. 33, pp. 161–172. https://doi.org/10.1016/j.mechatronics.2015.12.006
23. Xin, F., Chang-An, Z., Xiao-Ye, M., Hu, D. (2023). Resonance regulation on a hydraulic pipe via boundary excitations. *International Journal of Mechanical Sciences*, Vol. 252, 108375. https://doi.org/10.1016/j.ijmecsci.2023.108375
24. Fossen, T.I., Nijmeijer, H. (2012). *Parametric Resonance in Dynamical Systems*. Springer, New York, NY, USA. https://doi.org/10.1007/978-1-4614-1043-0
25. Mikota, G., Manhartsgruber, B., Kogler, H., Hammerle, F. (2017). Modal testing of hydraulic pipeline systems. *Journal of Sound and Vibration*, Vol. 409, pp. 256–273. https://doi.org/10.1016/j.jsv.2017.08.001
26. Stosiak, M. (2011). Vibration insulation of hydraulic system control components. *Archives of Civil and Mechanical Engineering*, Vol. 11(1), pp. 237–248. https://doi.org/10.1016/S1644-9665(12)60186-1
27. Urbanowicz, K., Bergant, A., Stosiak, M., Karpenko, M., Bogdevičius, M. (2023). Developments in analytical wall shear stress modelling for water hammer phenomena. *Journal of Sound and Vibration*, Vol. 562, 117848. https://doi.org/10.1016/j.jsv.2023.117848
28. Bingham, C., Stone, D.A., Schofield, N., Howe, D., Peel, D. (2000), Amplitude and frequency control of a vibratory pile driver. *IEEE Transactions on Industrial Electronics*, Vol. 47(3), pp. 623–631. https://doi.org/10.1109/41.847903
29. Zouari, F., Nasraoui, S., Louati, M., Ghidaoui, M.S. (2021). Transformation between damped and undamped waterhammer waves. *Journal of Sound and Vibration*, Vol. 491, 115706. https://doi.org/10.1016/j.jsv.2020.115706
30. Al-Habaibeh, A., Hamadeh, L., McCague, J. (2023). Experimental study for evaluating the response of the power take off of a point absorber wave energy generation system using a hydraulic wave simulator. *Ocean Engineering*, Vol. 281, 114906. https://doi.org/10.1016/j.oceaneng.2023.114906